Simulation of performance enhancement for water pollution sensor based on fiber optic technique

Cite as: AIP Conference Proceedings **2290**, 050032 (2020); https://doi.org/10.1063/5.0027513
Published Online: 04 December 2020

Maher Khaleel Ibrahim, Shehab A. Kadhim, and Nabeil Ibrahim Fawaz

Simulation of Performance Enhancement for Water Pollution Sensor Based on Fiber Optic Technique

Maher Khaleel Ibrahim [1, a)], Shehab A. Kadhim [2)], Nabeil Ibrahim Fawaz [1)]

[1]*Department of Physics, Collage of Science, University of Anbar, Anbar, Iraq*
[2]*Laser &Optoelectronics Research Center, Ministry of Science & Technology, Baghdad, Iraq*

[a)] Corresponding author: maheralani70@gmail.com

Abstract. Due to the increase in water pollution (Bacteria, viruses, heavy metals, salts, etc..), it became necessary to search for new technologies and develop their performance in detecting and sensing levels of pollution for the purpose of treating them. Here in this research paper, simulation, through the COMSOL software was performed to develop the performance of the optical fiber pollution sensor through the test of changing the parameters of the optical fiber structure such as the cladding diameter with different thicknesses and doping of its material, which was of silicon with germanium with different concentrations and studying the amount of better thickness and the best concentration of the impurity to obtain the best performance of the optical fiber sensor In sensing water pollution with sodium chloride salt (for example). A single mode optical fiber with different diameters had been designed as a pollution sensor. These sensors were doped with Germanium with different concentrations in cladding region. From the obtained results it had been found that the sensors with less diameter of nanometer range were more sensitive to refractive index change of applied analyte. The higher sensitivity was obtained with fiber diameter circa 6.5 μm. Also it had been found that as Germanium concentration increase (with fixed cladding thickness) the sensor were more sensitive to the change of analyte refractive index, the best results were obtained with concentration 0.19 wt%. These sensors could be very useful in field of water pollution detection.

Keywords: optical fiber sensor; Finite Element Method; Germanium doping; water pollution.

INTRODUCTION

Water is known to be contaminated if certain contaminants or factors are present to such an extent that the water cannot be used for a particular purpose. Water pollution is the presence in water of excessive amounts of a hazard (pollutants) so that it is not long suitable for eating, bathing, cooking or other uses [1].

Water pollution sensing plays an important role for industrial processes and the safety of health and control of chemical and biological studies. Because of the presence of sodium chloride, salinity calculation was carried out on the basis of the water refractive index. The electrical conductivity technique could be used, but this technique has significant drawbacks, such as the sensitivity to electromagnetic interference and the fact that other forms of contaminants will affect the sample's electrical conductivity leading to errors in the tests [2]. In addition, the performance of water-conductivity and water-density datasets has been linked to the fact that the refractive index (RI) with a density of 80 percent is better than conductivity because conductivity cannot detect species that can add to density but cannot be calculated by conducting electricity [3]. For these purposes, there has been a growing interest in fiber optic sensors due to their well-known compactness, high sensitivity, in situ measurement and tolerance to external electromagnetic interference [4].

From previous studies in this field:(Abhay Tambo and others 2008), The researcher developed a fiber-optic sensor based on LSPR. Naoparticles coated fibers are used in the design of sensors, and the sensor response to fluoride impurities in water was studied [5]. (Md. Faizul Huq Arif, Md. Jaminul Haque Biddut 2017), This paper proposes the design and optimisation of optical fiber microstructure for applications for liquid sensing. Numerical

The 8th International Conference on Applied Science and Technology (ICAST 2020)
AIP Conf. Proc. 2290, 050032-1–050032-9; https://doi.org/10.1063/5.0027513
Published by AIP Publishing. 978-0-7354-4020-3/$30.00

research is carried out using the Total Vector Finite Element Method (FEM) to analyze the modal birefringence, containment loss, relative sensitivity and nonlinear coefficient of the PCF structure proposed [6].

(Md. Shadidul Islam and others 2018), A rhombic shape core dependent photonic crystal fiber (RC-PCF) has been proposed in this paper for sensing purposes with aqueous analytes. The proposed RC-PCF structure was modeled on pure silica and numerically simulated in the finite element method (FEM) commercial software package COMSOL Multiphysics version 4.2 using perfectly matched anisotropic layering (A-PML) [7] .

(S.F.A.Z. Yusoffa , M.H. Mezhera , and others ,2018), A simulative analysis using COMSOL Multi Physics was also performed to research the relationship between the analyte on the different refractive index materials and the simulation study follows the finite element method (FEM) [8] .

In this work the optical propagation of such optical fiber sensors is simulated using COMSOL Multiphysics ® for a specific wavelength and different concentrations of solvents. The application of simulation follows the form Finite Elements (FEM). To investigate the efficiency of the optical fiber sensor, we modeled simulations using the COMSOL Multiphysics tool "Finite Element Method" (FEM). Optimum operating wavelength ranges for different concentrations of solvents are established, and techniques to introduce additional variables are implemented to further minimize optical losses.

THEORETICAL PART

Since Lukosz's first publication in 1983, Evanescent waveguides have been investigated a lot [9]. Several researchers have now built and demonstrated an optical waveguide sensing system based on evanescent sensing and these sensors are ideal for bio-chemical sensing. The waveguide uses evanescent waves around the surface of the waveguide to sense the refractive index change. A smart fiber optic sensor for measuring the concentration of salinity in solution has been built in one configuration of the optical fiber sensor. The sensor operates based on a step-by-step measurement process that involves submerging of the sensor's head, submersion, emergence and emergence from the solution being examined [10].

The calculated signal should focus on the solution's coefficient of surface tension, viscosity, turbidity and refraction. The variance in the amplitude of the measured signal against time provides information on the liquid type [11].

Changing boundary conditions is also directly related to changing the dimensions of optical fiber. The light is not propagated on the system core / cladding but the air / cladding interface. The approximations used for a typical optical fiber in the mode solutions, where the difference in refractive indices is low (less than 1%), are not valid. In this case, in the optical fiber concentrated, The light beam continues to be affected by the surrounding fiber — the light beam extends throughout the structure (as a core) and the surrounding area becomes a cladding as shown in fig 1 [12],[13]

Such an approach enables us to use additional material, especially in the taper waist zone, in a condensed area fig 1 . The optical fiber will be prone in this area to external changes in the reflective index of the material surrounding the fibre. These connections with various materials were commonly used for the construction of sensors, filters, and amplifier.

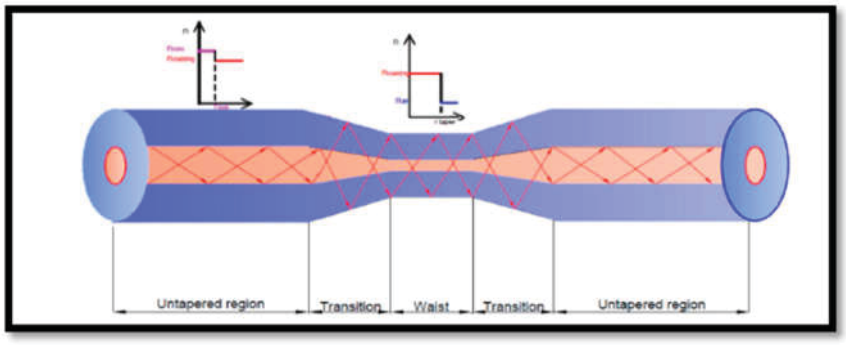

FIGURE 1. The scheme of light propagation in a tapered optical fiber—changes of boundary conditions

The thickness of the cladding within the fiber sensing area greatly impacts a Fiber Optic Evanescent Wave Sensor (FOEWS) response behavior. When the external media's Index of Refraction (IOR) is lower than that of the core, the incidence of rays at the core cladding interface creates an evanescent effect. The evanescent field attenuates

by means of the cladding and external media exponentially in amplitude away from the fiber core, without bringing energy away from the core. When the external analyte's IOR is equal to or greater than the core, the evanescent field within the cladding produces a propagating wave at the external analyte interface cladding that causes energy from the core to tunnel through the thin cladding and carries energy away from the center of the fiber.

Figure 2 indicates the shift in the FOEWS transmission range as a function of cladding thickness. The transmission range is defined as the measure of the decrease in transmission signal over the range of analyte IOR values from the reference power to the lowest transmitted power observed. The transmission range of the FOEWS as a function of cladding thickness show exponential activity from the graph of fig 2. This behavior can be exploited to assess the cladding thickness of manufactured sensors more accurately since it provides a relationship between cladding thickness and optical response without depending on the fiber's absolute transmission speed [13].

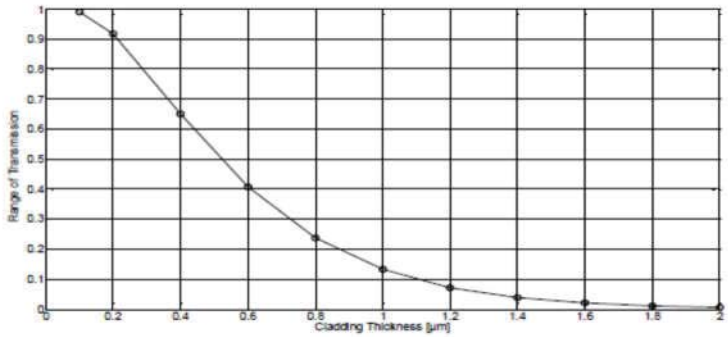

FIGURE 2. Prediction of the change in transmission range of the FOEWS response as a function of cladding thickness [13].

It is assumed that the core of optical fiber is constructed from fused silica. The refractive index of fused silica varies with wavelength according to the Sellmeier dispersion relationship as [14].

$$n_1(\lambda) = \sqrt{1 + \frac{a_1\lambda^2}{\lambda^2 - b_1^2} + \frac{a_2\lambda^2}{\lambda^2 - b_2^2} + \frac{a_3\lambda^2}{\lambda^2 - b_3^2}} \quad \text{.....(1)}$$

Where, λ is the wavelength in µm and a_1, a_2, a_3, b_1, b_2 and b_3 are Sellmeier coefficients. The values of these coefficients are given as, a_1 = 0.6961663, a_2 = 0.4079426, a_3 = 0.8974794, b_1 = 0.0684043

b_2 =0.1162414 and b_3 = 9.896161 .

The optical fiber's SiO2 core is usually doped with a GeO2 X standard. The calculation of the refractive index in pure silica and in a glass doped with an X percentage of GeO2 as a function of the wavelength follows the Sellmeier relationship according to equation 2 [14]:

$$n = \sqrt{1 + \sum_{i=1}^{3} \frac{[B_i^S + X(B_i^G - B_i^S)]\lambda^2}{\lambda^2 - [C_i^S + X(C_i^G - C_i^S)]^2}} \quad \text{.....(2)}$$

Where the Sellmeier coefficients are $B_i^S, B_i^G, C_i^S, and\ C_i^G$ and the S and G superscripts are SiO2 and GeO2, respectively[14].

The refractive index of the mixture consisting of water and sodium chloride can be calculated by following the Arago- Biot equation 3:

$$n - 1 = (n1 - 1)\, y1 + (n2 - 1)\, y2 \quad \text{.....(3)}$$

Where, n = Refractive index of mixture, n1 and n2 =Refractive index of water and sodium chloride respectively, y1and y2 = Volume fractions [15].

SIMULATION PART

The Finite Element Method (FEM) had been used to develop a software (COMSOL Metaphysics) simulated the present sensor. COMSOL Metaphysics ® is a software package of generic finite elements designed to address a wide range of physical phenomena.

COMSOL Metaphysics ® 4.4 Radio Frequency System was used to analyze mode and calculate optical losses. Once the geometries are set, refractive indices (real part and imaginary part) are given to the core and cladding materials at certain wavelength. Triangular meshing element was used. The test was done by COMSOL software on

the single mode of the optical fiber sensor, assuming that the core diameter of the fiber is 9 μm and the cladding diameter is 125 μm the propagation wavelength was 1.55 μm. Figure 3 shows the standard dimension of designed SMF.

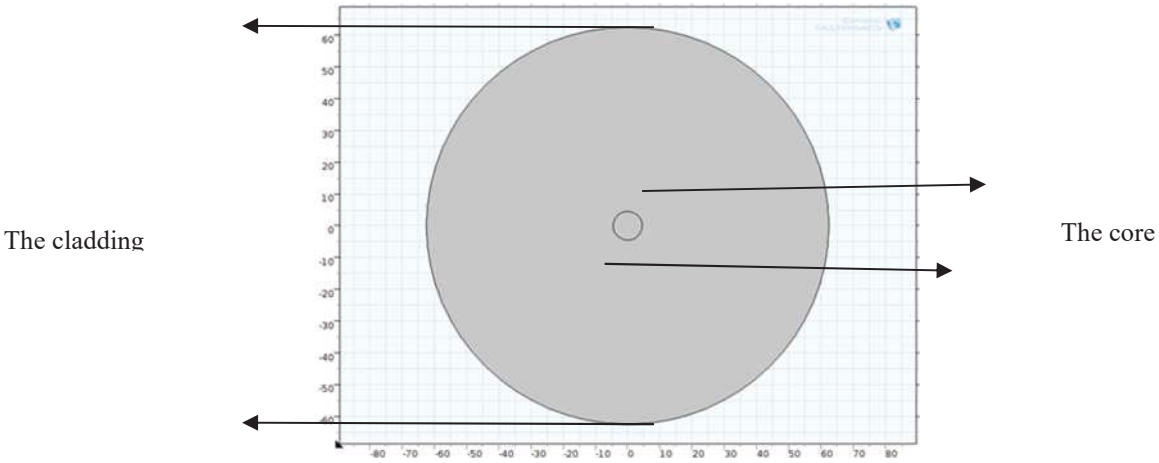

FIGURE 3. The designed SMF with standard dimensions.

The simulation model step was presented as flow chart, which is clear in Fig 4

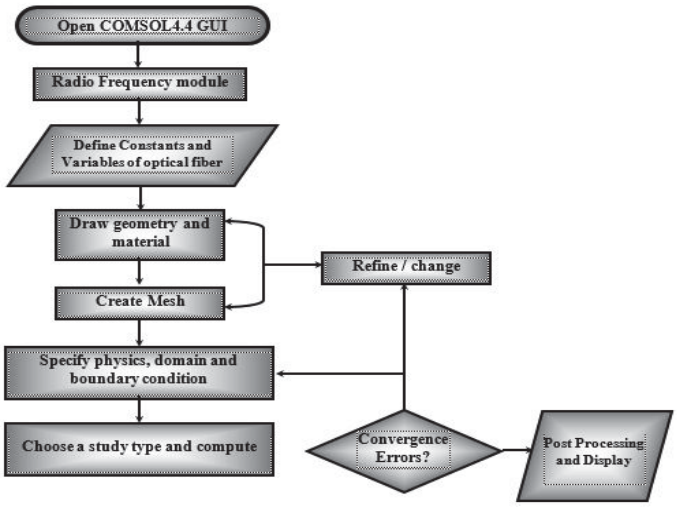

FIGURE 4. Flow chart represents the simulation steps for the designed sensor.

Different fiber diameters had been tested perform the characteristics of presented fiber sensors; we began from standard diameter of SMF which is 125 μm to 9.5 μm. The cladding of these fibers had been doped with different concentrations of GeO_2. The refractive indices of cladding after doping process had been calculated through equations 2 and 3. Then the designed sensors had been immersed into salty analyte which is sodium chloride. Different analyte concentration had been tested which was (0.1-0.5) wt%. The behavior of Eigen value which is the effective refractive index of the fundamental mode at 1.55 μm had been collected for different sensors.

RESULTS AND DISCUSSION

The light propagation of different fiber sensors had been presented in this section. From theoretical results, it was found that when the refractive index of pure silica fiber core was 1.444024 at propagation wavelength of 1.55 μm ,

the obtained effective refractive index for the fundamental mode was equal to 1.446247, which means that there are the light is tightly confine inside the core . While the value of the effective refractive index for the fundamental mode decreased at propagation wavelength of 1.55 µm in case of doped cladding with different concentrations.

For fiber diameter 125 µm. the higher variation of the fundamental mode of core was 1.444203 which is obtained at GeO_2 concentration 0.19 wt%. Then the effective refractive index returns to decrease. The different fundamental mode of the above cases had been illustrated in fig 5 a, b, &c respectively. While fig 6 shows the variation of effective refractive index versus GeO_2 concentration. Table 1 shows the values of effective refractive index for each GeO_2 concentration.

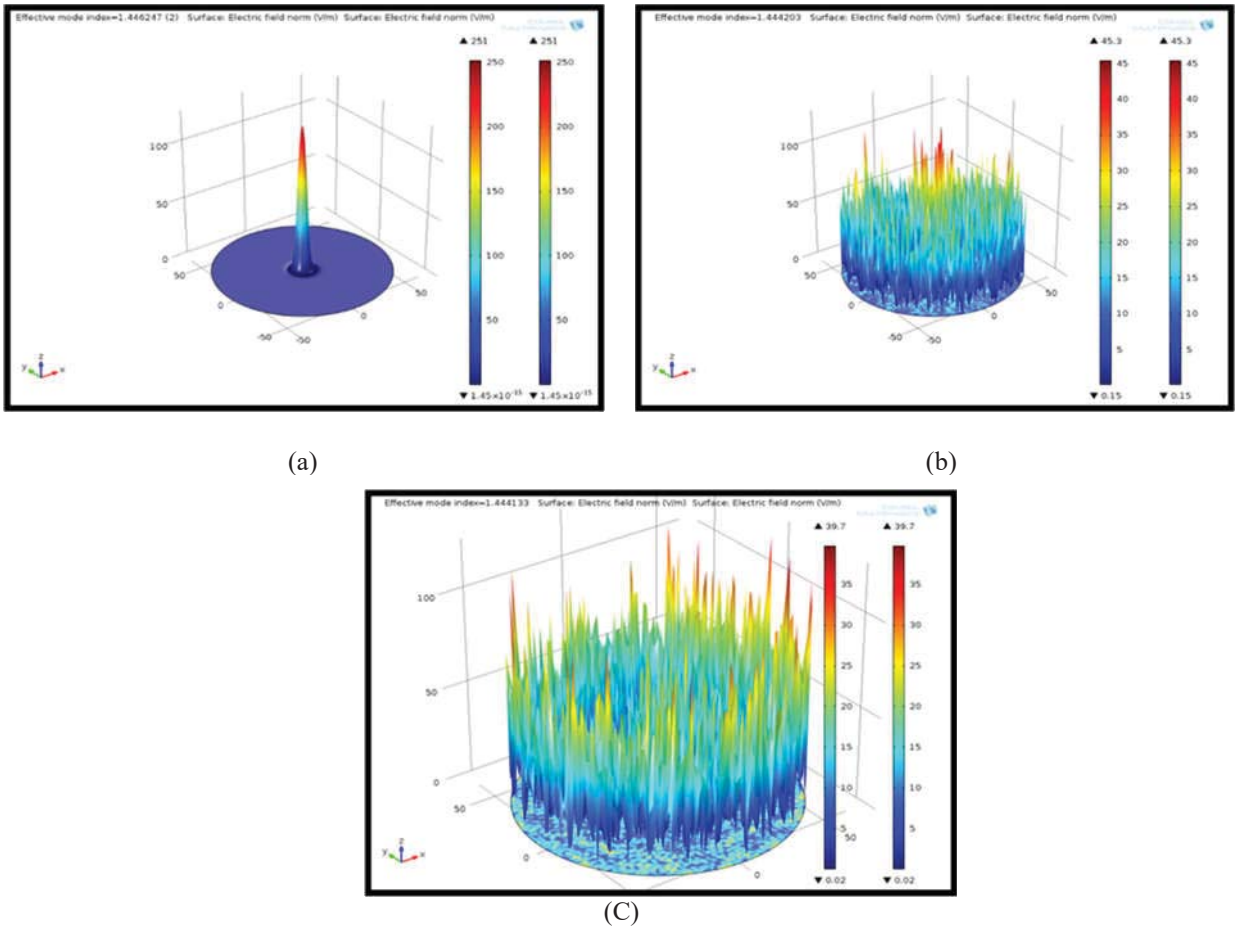

FIGURE 5. Fundamental mode of fiber optics sensor at 1.55 µm **(a)** pure silica, and doped fibers with GeO2 concentration of **(b)** 0.19 wt% and **(c)**0.25wt%**.**

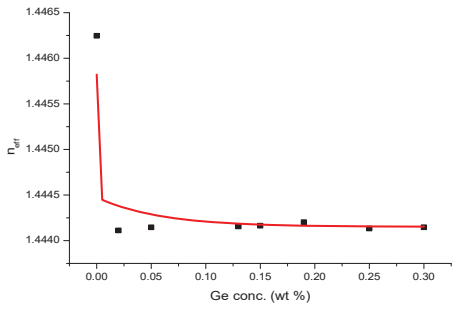

FIGURE 6. Variation the value of the effective refractive index with the concentration of GeO_2

TABLE 1. The Variation of the effective refractive index with the concentration of GeO_2 at the propagation wavelength 1.55μm.

Const. of GeO_2 (wt %) (cladding doped)	Cladding refractive index	Effective refractive index
0 (pure silica)	1.434024 (Assumption)	1.446247
0.02	1.447029601	1.444112
0.05	1.451526475	1.444146
0.13	1.463445766	1.444156
0.15	1.466409446	1.444164
0.19	1.472317821	1.444203
0.25	1.481133712	1.444133
0.3	1.48843839	1.444147

Figure 7 shows the behavior of effective refractive index due to reduce of fiber diameter to each for all cases of GeO_2 concentration cladding doping . From the results we can notice that when the optical fiber was immersed in sodium chloride solution with concentrations from 0.1 to 0.5 (wt %) and the doping percentage of GeO2 in the cladding material was 0.02 with reducing the thickness of the cladding. The higher variation of effective refractive index was obtained at cladding thickness equal to 0.25 μm or (fiber diameter 4.75μm) where the value of the effective refractive index coefficient changed from 1.445421 to 1.446137.

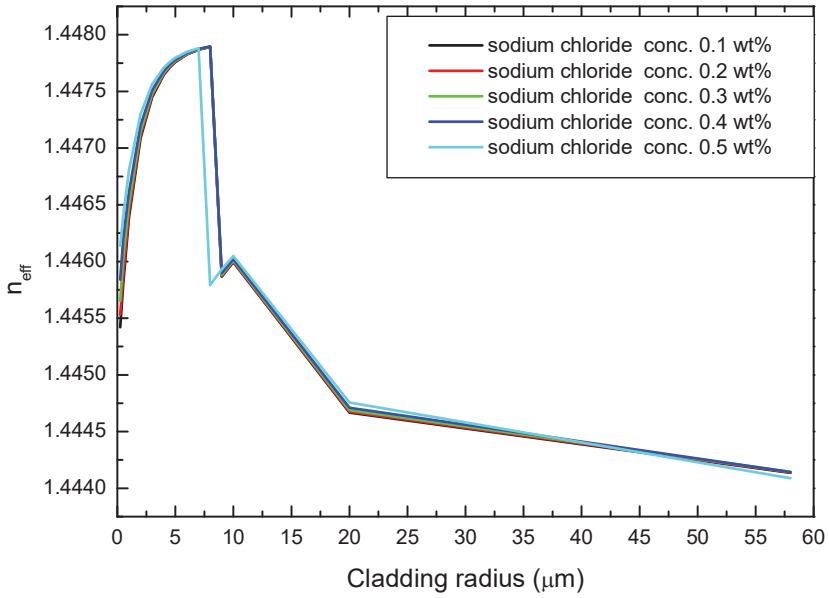

FIGURE 7. The behavior of the effective refractive index with the cladding radius of different concentration of sodium chloride and GeO2 concentration of 0.02 wt%

Table 2 shows the values of effective refractive for each case at propagation wavelength 1.55 μm.

TABLE 2. The variation of the effective refractive index with the cladding radius at 0.02 wt% GeO2concentration for the propagation wavelength 1.55 μm.

Cladding radius (μm)	n_{eff} for NaCl conc. 0.1 wt%	n_{eff} for NaCl conc. 0.2 wt%	n_{eff} for NaCl conc. 0.3 wt%	n_{eff} for NaCl conc. 0.4 wt%	n_{eff} for NaCl conc. 0.5 wt%
58	1.444136	1.444141	1.444144	1.444143	1.444088
10	1.445994	1.446	1.446008	1.446021	1.446048
5	1.447759	1.447764	1.44777	1.447779	1.447797
2	1.447088	1.447114	1.447148	1.447201	1.447299
1	1.446388	1.446435	1.446508	1.446612	1.446804
0.25	1.445421	1.44553	1.445653	1.44584	1.446137

The higher variation of effective refractive index had been obtained for the GeO_2 doping percentage equal to 0.13 wt%, and cladding thickness equal to 2 μm or (fiber diameter 6.5μm) where the effective refractive index changed from 1.451135 to 1.452579, as shown in Fig 8 and table 3.

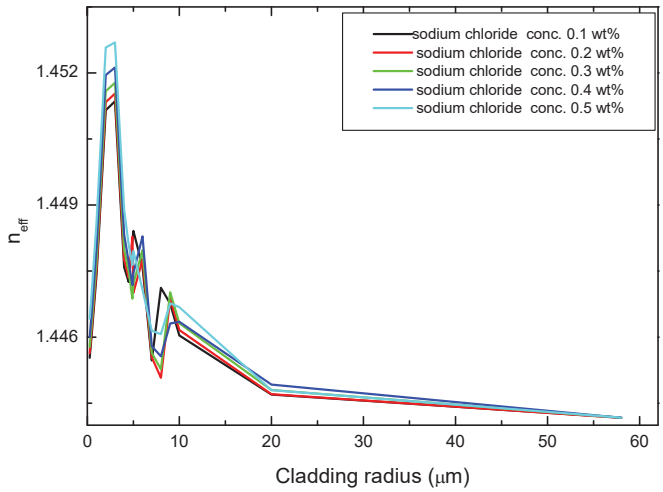

FIGURE 8. The behavior of the effective refractive index with the cladding radius of different concentration of sodium chloride and GeO_2 concentration of 0.13 wt%.

TABLE 3. The variation of the effective refractive index with the cladding radius at 0.13 wt% GeO2concentration for the propagation wavelength 1.55 μm.

Cladding radius (μm)	n_{eff} for NaCl conc. 0.1 wt%	n_{eff} for NaCl conc. 0.2 wt%	n_{eff} for NaCl conc. 0.3 wt%	n_{eff} for NaCl conc. 0.4 wt%	n_{eff} for NaCl conc. 0.5 wt%
58	1.44417	1.444165	1.444167	1.444169	1.444172
10	1.446039	1.44616	1.446315	1.446350	1.446681

Cladding radius (μm)	n_{eff} for NaCl conc. 0.1 wt%	n_{eff} for NaCl conc. 0.2 wt%	n_{eff} for NaCl conc. 0.3 wt%	n_{eff} for NaCl conc. 0.4 wt%	n_{eff} for NaCl conc. 0.5 wt%
5	1.448413	1.447007	1.447212	1.447453	1.447953
2	1.451153	1.451336	1.451585	1.451952	1.452579
1	1.44611	1.447569	1.447762	1.448064	1.447066
0.25	1.445531	1.445634	1.445778	1.446000	1.446416

When the GeO_2 doping percentage was 0.19, the best case of fiber optic sensitivity when increasing the salt concentration from 0.1 to 0.5 (wt %) at cladding thickness equal to 2 μm or (fiber diameter 6.5μm) where the effective refractive index changed from 1.452083 to 1.454629 as in Fig 9 and table 4.

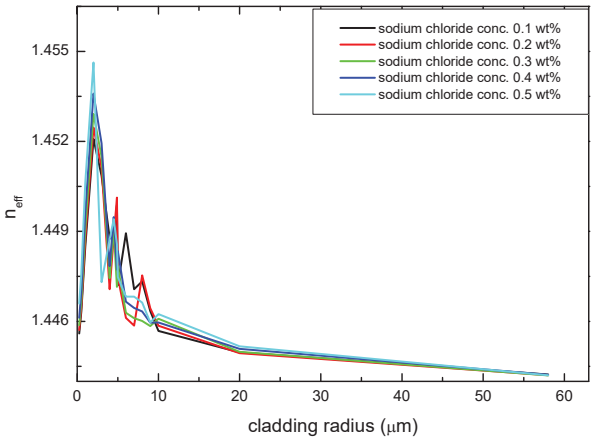

FIGURE 9. The behavior of the effective refractive index with the cladding radius of different concentration of sodium chloride and GeO2 concentration of 0.19 wt%.

TABLE 4. The variation of the effective refractive index with the cladding radius at 0.19 wt% GeO2concentration for the propagation wavelength 1.55 μm.

Cladding radius (μm)	n_{eff} for NaCl conc. 0.1 wt%	n_{eff} for NaCl conc. 0.2 wt%	n_{eff} for NaCl conc. 0.3 wt%	n_{eff} for NaCl conc. 0.4 wt%	n_{eff} for NaCl conc. 0.5 wt%
58	1.44423	1.444208	1.444201	1.44422	1.444203
10	1.445681	1.445856	1.446089	1.445961	1.446244
5	1.447204	1.447476	1.447835	1.448342	1.447478
2	1.452083	1.45246	1.452914	1.453593	1.454629
1um	1.4485	1.448747	1.449096	1.449642	1.45064
0.25	1.445597	1.445712	1.445872	1.446121	1.446596

CONCLUSIONS

In this work an optical fiber sensor performance characteristic had been submitted. This fiber had been designed for water pollution purpose. Single mode fiber had been designed using finite element method. The designed sensors had been immersed in sodium chloride analyte with different concentrations. Two parameters had been analyzed to study the performance of the sensor; fiber diameter and doping concentration. We found that when the fiber diameter reduced to 6.5 μm we gate higher variation of effective refractive index. Also, when the cladding of these fibers had been doped with germanium with different concentration the variation of effective refractive index improved thus the sensitivity of sensor improved too. These results could be very effective in field of water pollution sensors.

REFERENCES

1. Owe, F.D., 2013. Water pollution: Sources, effects, control and management. Mediterranean Journal of Social Sciences, 4(8), p.65.
2. Lopez, O., Garcia, M.A., Gomes, D., Rojas, P., Sospedra, J. and Sánchez-Arcilla, A., 1999. Hydrographic and hydrodynamic characteristics of the eastern basin of the Bran field Strait (Antarctica). Deep Sea Research Part I: Oceanographic Research Papers, 46(10), pp.1755-1778.
3. Millard, R.C. and Saver, G., 1990. An index of refraction algorithm for seawater over temperature, pressure, salinity, density, and wavelength. Deep Sea Research Part A. Oceanographic Research Papers, 37(12), pp.1909-1926.
4. Cong, J., Zhang, X., Chen, K. and Xu, J., 2002. Fiber optic Bragg grating sensor based on hydro gels for measuring salinity. Sensors and Actuators B: Chemical, 87(3), pp.487-490.
5. Tambo, A., Kumbhaj, S., Lalla, N.P. and Sen, P., 2016, October. LSPR based fiber optic sensor for fluoride impurity sensing in potable water. In Journal of Physics: Conference Series (Vol. 755, No. 1, p. 012058). IOP Publishing.
6. Arif, M.F.H. and Biddut, M.J.H., 2017. A new structure of photonic crystal fiber with high sensitivity, high nonlinearity, high birefringence and low confinement loss for liquid analyte sensing applications. Sensing and Bio-Sensing Research, 12, pp.8-14.
7. Islam, M.S., Paul, B.K., Ahmed, K. and Asaduzzaman, S., 2018. Rhombic core photonic crystal fiber for sensing applications: Modeling and analysis. Optic, 157, pp.1357-1365.
8. Yusuf, S.F.A.Z., Mezher, M.H., Amiri, I.S., Ayyanar, N., Vigneswaran, D., Ahmad, H. and Zakaria, R., 2018. Detection of moisture content in transformer oil using platinum coated on D-shaped optical fiber. Optical Fiber Technology, 45, pp.115-121.
9. Lukosz, W. and Tiefenthaler, K., 1983, October. Directional switching in planar waveguides effected by adsorption-desorption processes. In Institution of Electrical Engineers. 2nd European Conference of Integrated Optics (pp. 17-18).
10. Borecki, M., 2007. Intelligent fiber optic sensor for estimating the concentration of a mixture-design and working principle. Sensors, 7(3), pp.384-399.
11. Borecki, M. and Kruszewski, J., 2001. Intelligent high resolution sensor for detecting of liquid mediums. Optical Applicata, 31(4), pp.691-700.
12. Brambilla, G., 2010. Optical fiber nanowires and microwires: a review. Journal of Optics, 12(4), p.043001.
13. Godin, J.R., 2015. Development of an Analytical Model for a Fiber Optic Evanescent Wave Sensor.
14. Santos, D. F. D. N. D. (2017). A numerical approach into new designs for SPR sensors in D-type optical fibers.
15. Arif, M.F.H., Biddut, M.J.H., Babu, M.S.I., Rahman, H.M., Rahman, M.M., Jahan, B., Chaity, M.S. and Khaled, S.M., 2017. Photonic Crystal Fiber Based Sensor for Detecting Binary Liquid Mixture. Optics and Photonics Journal, 7(11), pp.221-234.